CONF-8810182--17

CONF-8810182--17

DE89 007379

September 30, 1988

Soller Collimators for Small Angle Neutron Scattering*

R. K. Crawford, J. E. Epperson, and P. Thiyagarajan
Argonne National Laboratory

Paper prepared for ICANS X

held at Los Alamos
October 3-7, 1988

*Work supported by U.S. Department of Energy, BES, contract No. W-31-109-ENG-38

Soller Collimators for Small Angle Neutron Scattering*

R. K. Crawford, J. E. Epperson, and P. Thiyagarajan
Argonne National Laboratory

The Collimation System at the IPNS Small Angle Diffractometer

Small angle diffractometers at pulsed sources need to have fairly short flight paths if they are to make use of the long-wavelength portion of the spectrum without encountering problems from frame overlap or sacrificing intensity with band-limiting or pulse-removing choppers. With such short flight paths, achieving the necessary angular collimation in the incident beam while utilizing the full source size (~ 10 cm diameter) and a reasonable sample size (~ 1 cm diameter) requires the use of converging multiple-aperture collimation.[1] If the collimation channels are all focused to the same point on the detector, then the large sample size will not affect Q_{min} or the Q-resolution,[2] even if the sample-to-detector distance is short. The Small Angle Diffractometer (SAD) at IPNS uses crossed converging soller collimators to provide focusing multiple-aperture collimation having ~ 400 converging beam channels with essentially no "dead" space between them. This entire collimator system occupies a distance of only ~ 60 cm along the incident flight path, while providing angular collimation of 0.003 radians FWHM. These collimators are shown schematically in Fig. 1. The dimensions for the SAD upstream collimator are L_c = 32.8 cm, d_1 = 0.974 mm, d_2 = 0.851 mm, while for the SAD downstream collimator L_c = 25.0 cm, d_1 = 0.844 mm, d_2 = 0.750 mm. Each of these collimators has 20 blades defining 21 horizontal or vertical channels.

*Work supported by U.S. Department of Energy, BES, contract No. W-31-109-ENG-38

These collimators use blades of stretched mylar coated with ^{10}B in a suitable binder,[3] and are commercially available (Cidic, Ltd., Cheltenham, England). For the initial set of such collimators provided to IPNS for SAD, the coating was brushed on in a layer ~ 10 microns thick on each side of the mylar. This set of collimators had adequate absorbing power to define the beam quite cleanly at the calculated geometrical limits when using 1 Å neutrons. However, at longer wavelengths "wings" began to appear on the transmission pattern, resulting in appreciable intensity appearing at the detector well outside the geometrical beam penumbra. Figure 2 shows a typical pattern of these "wings", with no sample or other scatterer in the beam, and Fig. 3 shows how the total "wing" intensity outside the beamstop (which was slightly larger than the geometrical beam penumbra) varied with wavelength. Note that even in the worst case the "wing" intensity was only ~ 3×10^{-5} of the main beam intensity, so although this collimator-produced background was large enough to be easily seen on the SAD and to interfere with the lowest Q data from weakly-scattering samples, this was really a very small effect.

Reflectivities of Absorbing Materials

The wavelength dependence exhibited in Fig. 3 suggested that this "wing" phenomena was probably due to reflections from the collimator blades. The reflectivity R of a flat surface of homogeneous material is given by[4]

$$R = \left| \frac{1 - \sqrt{(n^2 - \cos^2\theta)/\sin^2\theta}}{1 + \sqrt{(n^2 - \cos^2\theta)/\sin^2\theta}} \right|^2 \qquad (1)$$

where θ is the angle of incidence, and the complex index of refraction n can be written as

$$n^2 = n_r^2 - n_i^2 + i2n_r n_i$$

$$\simeq 1 - \frac{N\lambda^2}{\pi} \bar{b}_r + i \frac{N\lambda^2}{\pi} \bar{b}_i \qquad (2)$$

where $\bar{b}_r$ and $\bar{b}_i$ are the average real and imaginary components of the scattering

length for the material, and N is the number density of the material. Applying Eq. (2) to Eq. (1) and assuming that θ is small leads to

$$R = \frac{1 - 2[(E + \sqrt{E^2+F^2})/2]^{1/2} + \sqrt{E^2+F^2}}{1 + 2[(E + \sqrt{E^2+F^2})/2]^{1/2} + \sqrt{E^2+F^2}} \tag{3}$$

with

$$E = 1 - \frac{N\lambda^2}{\pi \sin^2\theta} \bar{b}_r \tag{4}$$

$$F = \frac{N\lambda^2}{\pi \sin^2\theta} \bar{b}_i \tag{5}$$

The "critical angle" θ_c is the angle which makes E = 0.

$$\sin^2\theta_c = \frac{N\lambda^2}{\pi} \bar{b}_r \tag{6}$$

In the case where F = 0 (no absorption), R = 1 for angles less than θ_c, and total reflection occurs. If $\bar{b}_r < 0$, θ_c is not defined and total reflection does not occur. However the reflectivity always approaches 1 as θ approaches 0 or λ approaches ∞, so it can still be substantial at small angles or large wavelengths.

Figure 4 shows the minimum reflectivity which results from varying E at constant F, as a function of F. Two features can be noted: 1) Very small reflectivities can only be obtained for F near 0, and hence for small values of $\bar{b}_i$ (implying small total cross-section) and/or small wavelengths and/or large angles. This means that within the framework of this theory, namely treatment of the medium as homogeneous and ignoring resonance effects, every good absorber is also at least a fairly good reflector at small angles and/or large wavelengths. 2) For any given F there is an optimum value for E, and hence for any given $\bar{b}_i$ there is an optimum value of $\bar{b}_r$ which will minimize the reflectivity. Thus there is some room for optimization by changing the material constituents to vary $\bar{b}_r$ even when $\bar{b}_i$ must remain large and fixed (as is the case when a material of a certain total absorption is required, but it is desired that this material have as low reflectivity as possible.)

A large value for the absorption cross-section leads to a large magnitude for $\bar{b}_i$, and hence to a large value for F, giving a relatively large reflectivity. Thus it is desirable to have a value for $\bar{b}_i$ no larger than necessary, as determined by the total absorption required. The best that could be done to minimize the reflectivity (within the framework of this homogeneous model) for the SAD collimators, while still providing adequate absorption, would be to coat them with a material having the approximate parameters

$$N\bar{b}_i \sim -1.4 \times 10^{9}\ \text{cm}^{-2} \tag{7}$$

$$N\bar{b}_r \sim -(2\text{-}8) \times 10^{8}\ \text{cm}^{-2} \tag{8}$$

Monte Carlo Simulation of Soller Collimators

The Monte Carlo simulation program SOLLER was written to simulate the transmission of neutrons through a converging or straight soller collimator. The program simulates just one channel of such a collimator, and treats the problem in two dimensions only. The blade surfaces were simulated by randomly chosen connected straight line segments. Because it was found that a few individual facets which were properly oriented for reflection could cause pronounced features in the pattern observed on the detector, new surfaces were generated several times during the simulation so that the results were averaged over different sets of surfaces. Both reflection probabilities, given by Eq. (3), and scattering probabilities were considered whenever a neutron path intersected one of these surfaces.

The downstream SAD collimator was simulated using the dimensions given above, and with the material parameters $\bar{b}_r = -0.0221 \times 10^{-12}$ cm, $\bar{b}_i = (-0.0556 - 0.00141/\lambda) \times 10^{-12}$ cm, $\bar{\sigma}_{inc} = 26.73$ barns, and $N = 1.222 \times 10^{23}$ per cm^3. (These parameters were derived on the assumption of a 50-50 (by volume) mixture of ^{10}B and CH_2, the latter simulating the binder.) A smooth surface and two different rough surfaces were simulated. For the rough surfaces the ends of the surface segments were allowed to vary $\pm$ 0.02 mm from the nominal surface line, and the mean surface segment lengths were set to 0.2 mm (0.1 rough) and 0.04 mm (0.5 rough) respectively (the second case being the "rougher" surface, with the rms angular variation of surface segments in the

second being 5 times that in the first). A "roughness" value is defined here as the ratio of maximum segment end displacement to mean segment length.

Figure 5 shows the ratios of the calculated "wing" probabilities to the main beam probabilities as functions of wavelength for each of these three surface roughness cases. For wavelengths > 2 Å, the collimator-produced background was due almost entirely to reflection from the blade surface facets, while for wavelengths < 2 Å incoherent scattering from the blade surfaces began to dominate. Also shown in Fig. 5 are the ratio of "wing" events to main beam events observed for the real SAD collimator. The 0.5 rough surface produced an absolute magnitude and a shape versus λ for the "wing" background very similar to that experimentally observed at SAD. (Simulated segment sizes in the 0.5 rough case approached realistic physical dimensions, with a 40 μ average length and a ± 20 μ maximum end displacement.)

The "wing" background fraction was also calculated using the SOLLER program for a 0.1 rough surface with the "optimized" parameters of Eqs. (7-8). A factor of 10-20 decrease in this background fraction, relative to that calculated above for the same roughness with the 50-50 mixture, was obtained by the use of the optimized materials, but small shifts ($\pm$ 0.004 x 10^{-12} cm) in $\bar{b}_r$ from the optimum value resulted in a factor of ~ 2 increase in the calculated collimator-produced background. Thus although significant gains can be achieved by optimizing the material parameters, these parameters must be adjusted quite close to the optimum values in order for these gains to be realized.

As can be seen in Fig. 5, surface roughness had a pronounced effect on the number of neutrons reflected out of the beam by the collimators. A decrease in "roughness" from 0.5 to 0.1 resulted in more than a factor of 10 increase in the "wing" background fraction, and the further decrease in roughness from 0.1 to 0.0 (smooth) increased this fraction by another factor of ~ 50. However there was very little change in the wavelength dependence of these fractions except for $\lambda \leq 2$ Å, where the incoherent scattering starts to dominate the results.

New Collimators

Based on the results of the Monte Carlo simulations and on the considerations of reflectivities of practical absorbing materials, it was concluded that significant improvements in soller collimator performance would be easier to achieve by improving the surface roughness, rather than by optimizing the absorbing coatings to minimize reflectivity. Fortunately, in the interim Cidic had developed a method for applying "matte" coatings, rather than the original brushed coatings, of the ^{10}B-plus-binder to the surfaces of their mylar collimator blades. Thus a second set of collimators was obtained, geometrically identical to the first SAD collimators but this time with the boron applied in two matte-finish coatings on each surface. These new collimator blade surfaces appeared distinctly rougher, and had significantly less optical "shine" than did the originals when viewed at grazing incidence. These new collimators were installed on SAD in May, 1988, and were much improved over the originals. No "wings" could be observed at all, and the background over the remainder of the detector was reduced as well. Figure 6 compares the "wing" background (obtained by integrating over the same set of detector cells used for calculating the original "wing" intensities) observed with these new collimators to that produced by the originals. Further testing of these new collimators will occur in Fall, 1988, but it is already clear that the rough surface has resulted in a significant improvement beam quality with no measurable reduction in main-beam intensity.

Summary

The neutron beam transmitted through the soller collimators on the SAD instrument at IPNS showed "wings" about the main beam. These "wings" were quite weak, but were sufficient to interfere with the low-Q scattering data. General considerations of the theory of reflection from homogeneous absorbing media, combined with the results from a Monte Carlo simulation, suggested that these "wings" were due to specular reflection of neutrons from the absorbing material on the surfaces of the collimator blades. The simulations showed that "roughness" of the surface was extremely important, with "wing" background variations of three orders of magnitude being observed with the range of roughness values used in the simulations.

Based on the results of these simulations, new collimators for SAD were produced with a much rougher ^{10}B-binder surface coating on the blades. These new collimators were determined to be significantly better than the original SAD collimators. This work suggests that any soller collimators designed for use with long wavelengths should be fabricated with such a rough surface coating, in order to eliminate (or at least minimize) the undesirable reflection effects which otherwise seem certain to occur.

REFERENCES

1. R. K. Crawford and J. M. Carpenter. J. Appl. Cryst., in press, (1988).

2. A. C. Nunes. Nucl. Instrum. Methods 119, 291-293 (1974).

3. C. J. Carlile, J. Penfold, and W. G. Williams. J. Phys. E: Sci. Instrum 11, 837-838 (1978).

4. G. E. Bacon. Neutron Diffraction, Third Edition. Clarendon Press. 1975.

FIGURE CAPTIONS

Fig. 1 Schematic representation of a crossed converging soller collimator system.

Fig. 2 Contour plot of total empty-beam background intensity on the SAD detector, showing the background "wings" observed about the main transmitted beam. The main beam has been absorbed by a beamstop and so is not seen in this figure.

Fig. 3 Observed ratio of collimator-produced "wing" background to main beam intensity for the original SAD soller collimators.

Fig. 4 Minimum reflectivity resulting from varying E (related to the real component of the scattering length - see text) at constant F (related to the imaginary component of the scattering length - see text) as a function of F.

Fig. 5 Monte Carlo simulation of collimator-produced "wing" background with different blade surface roughnesses and different material parameters. Solid - smooth blade surface; dotted - 0.1 rough blade surface; dashed - 0.5 rough blade surface; chain-dot - observed behavior for the original SAD collimators, taken from Fig. 3.

Fig. 6 Measured ratio of collimator-produced "wing" background to main beam intensity (triangles) for the new "rough-surface" SAD collimators. The observed behavior (circles) of the original SAD collimators is shown for comparison.

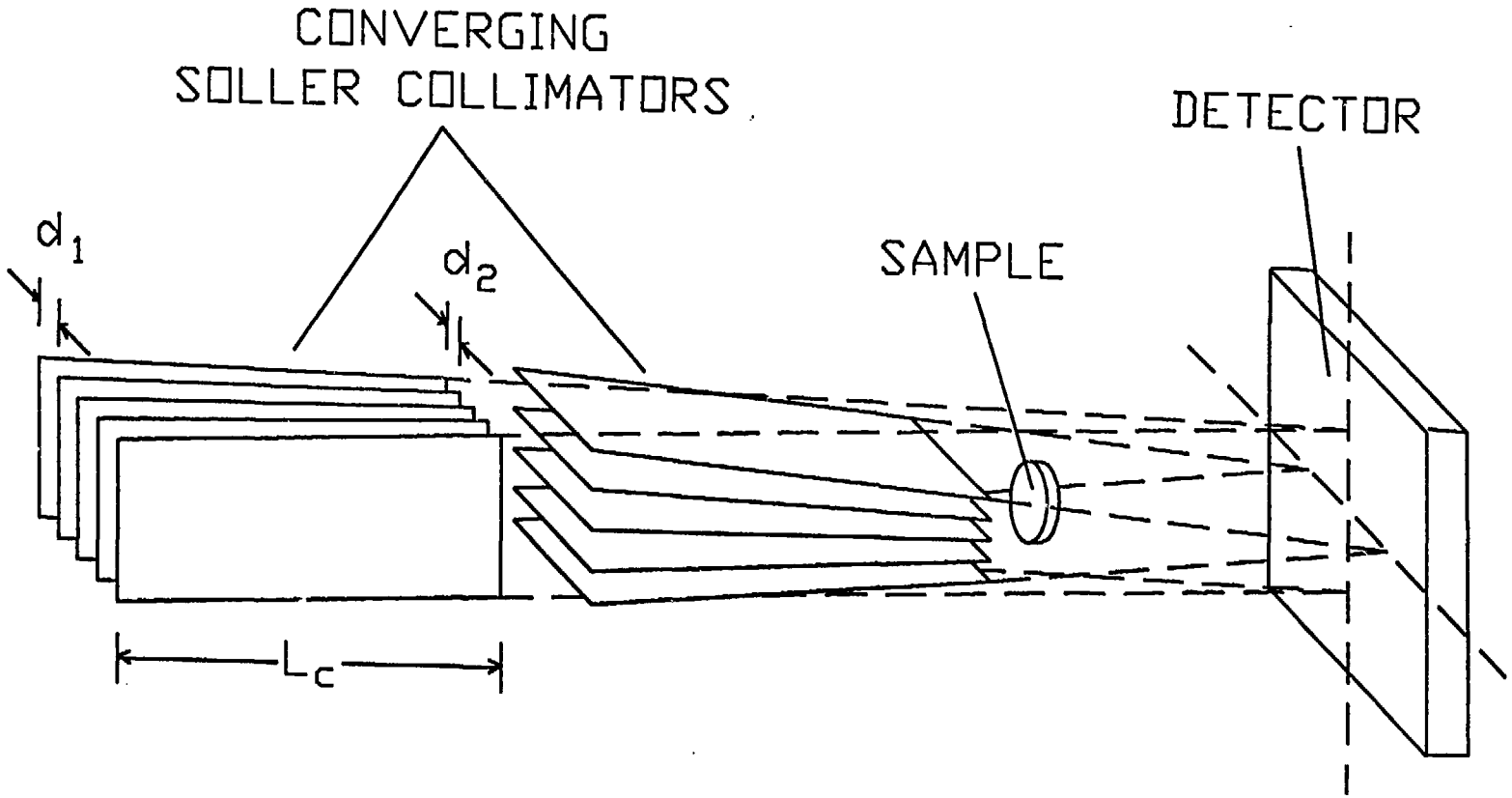
CONVERGING
SOLLER COLLIMATORS
DETECTOR
d_1
d_2
SAMPLE
L_c

Fig 2

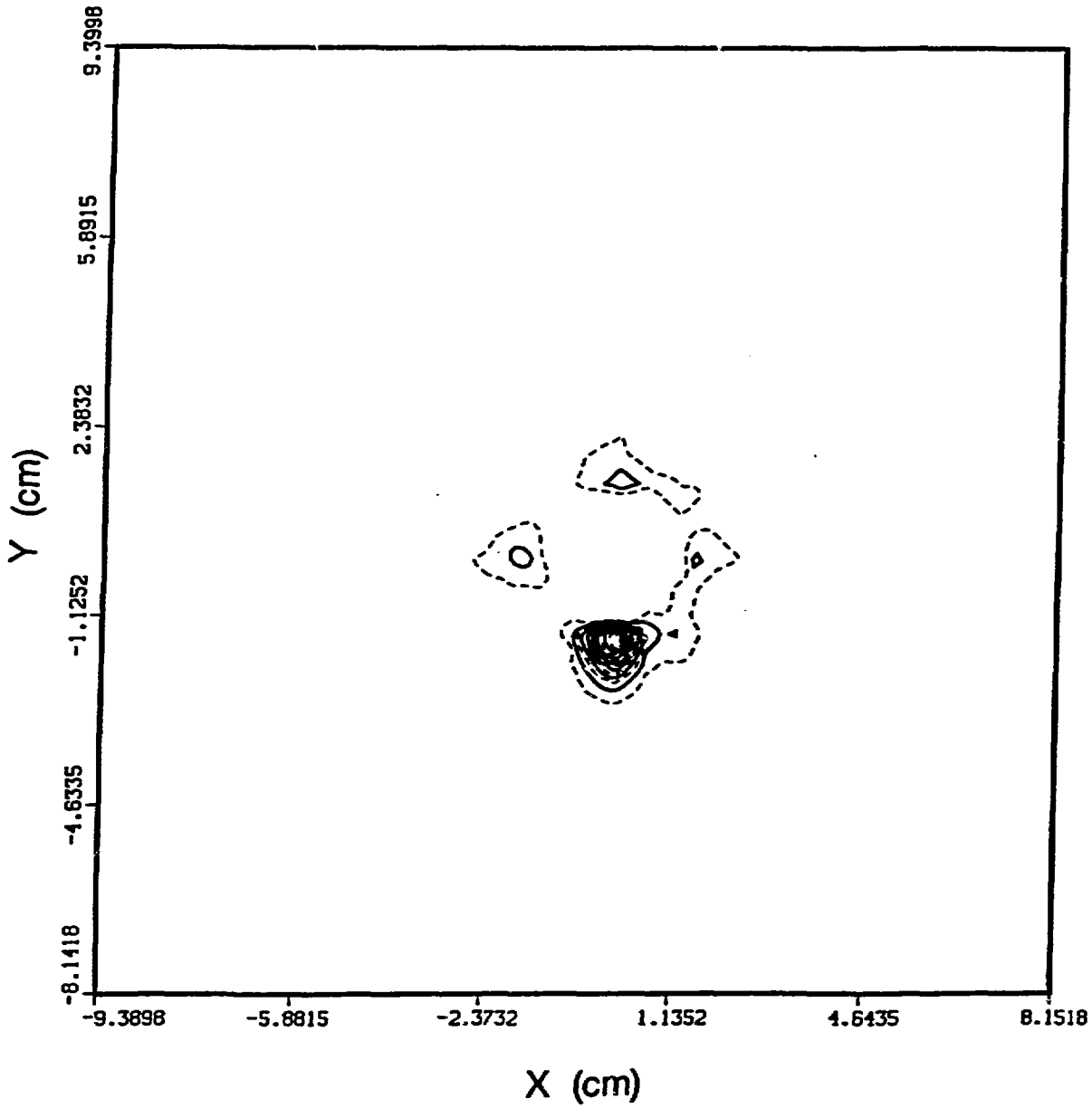
9.3998
5.8915
2.3832
-1.1252
-4.6335
-8.1418
Y (cm)
-9.3898
-5.8815
-2.3732
1.1352
4.6435
8.1518
X (cm)

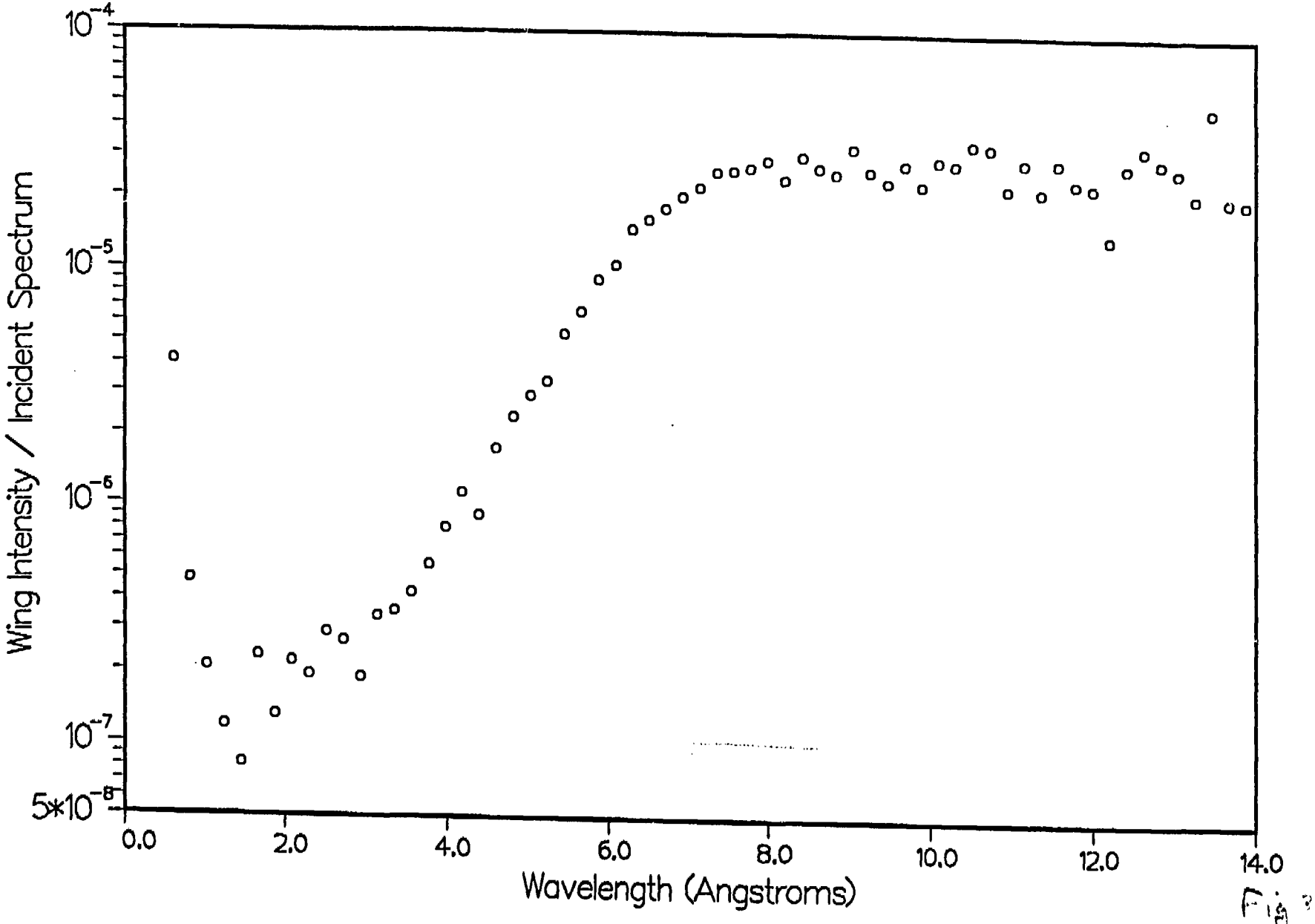
10^{-4}
10^{-5}
10^{-6}
10^{-7}
$5*10^{-8}$
Wing Intensity / Incident Spectrum
0.0
2.0
4.0
6.0
8.0
10.0
12.0
14.0
Wavelength (Angstroms)

Fig

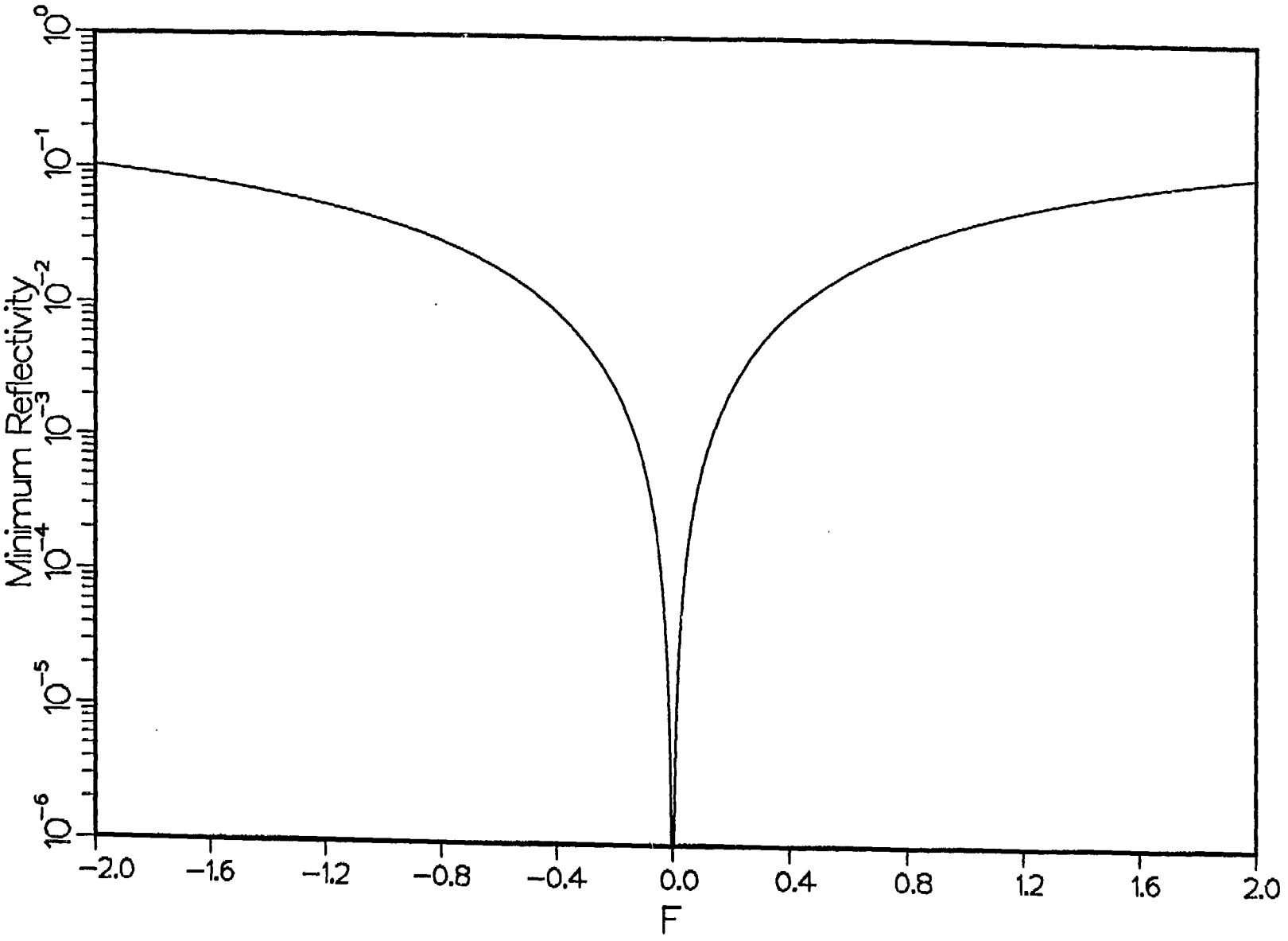
Minimum Reflectivity
10^{0}
10^{-1}
10^{-2}
10^{-3}
10^{-4}
10^{-5}
10^{-6}
−2.0
−1.6
−1.2
−0.8
−0.4
0.0
0.4
0.8
1.2
1.6
2.0
F

Fig 4

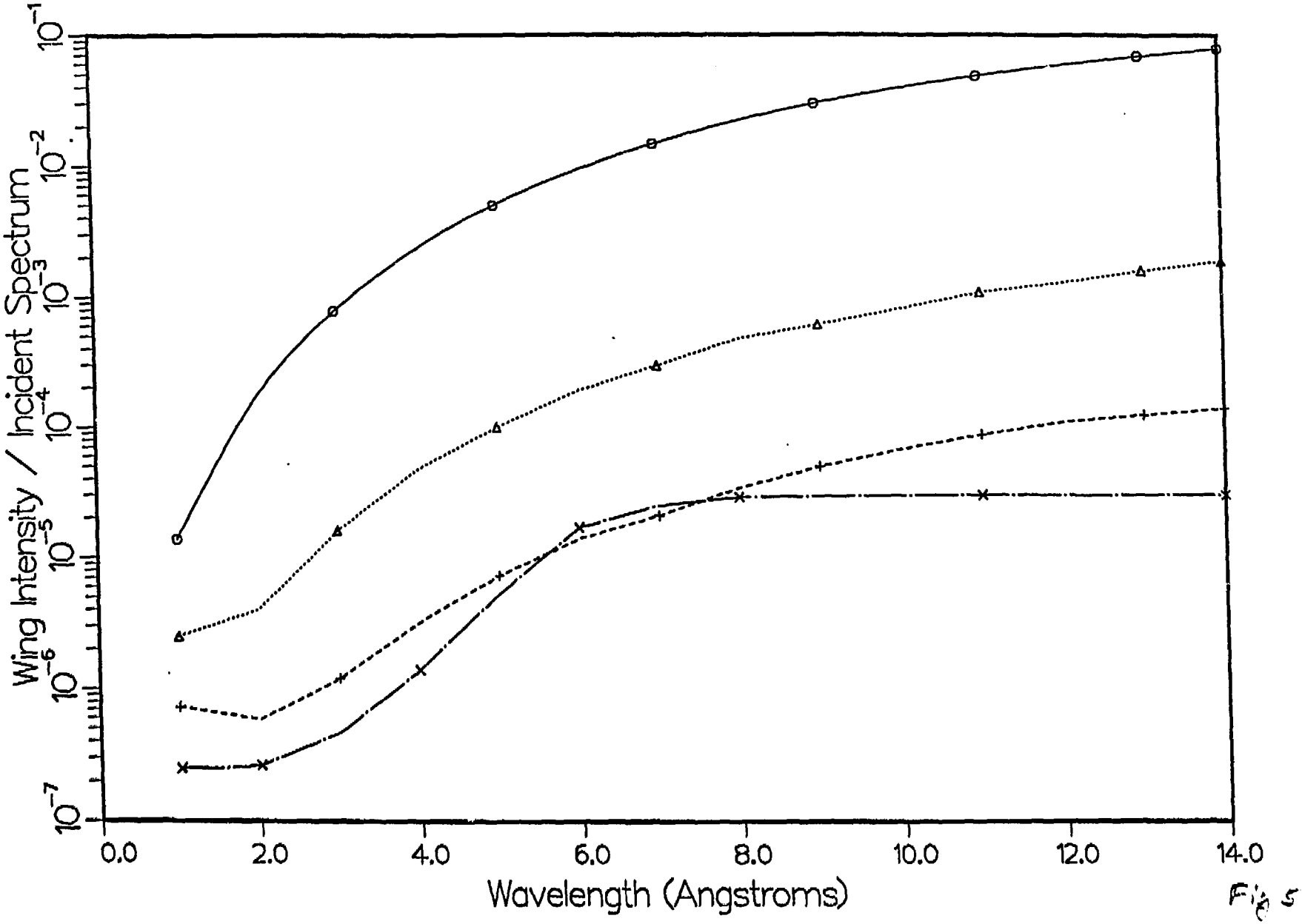
Wing Intensity / Incident Spectrum
10^{-1}
10^{-2}
10^{-3}
10^{-4}
10^{-5}
10^{-6}
10^{-7}
0.0
2.0
4.0
6.0
8.0
10.0
12.0
14.0
Wavelength (Angstroms)

Fig 5

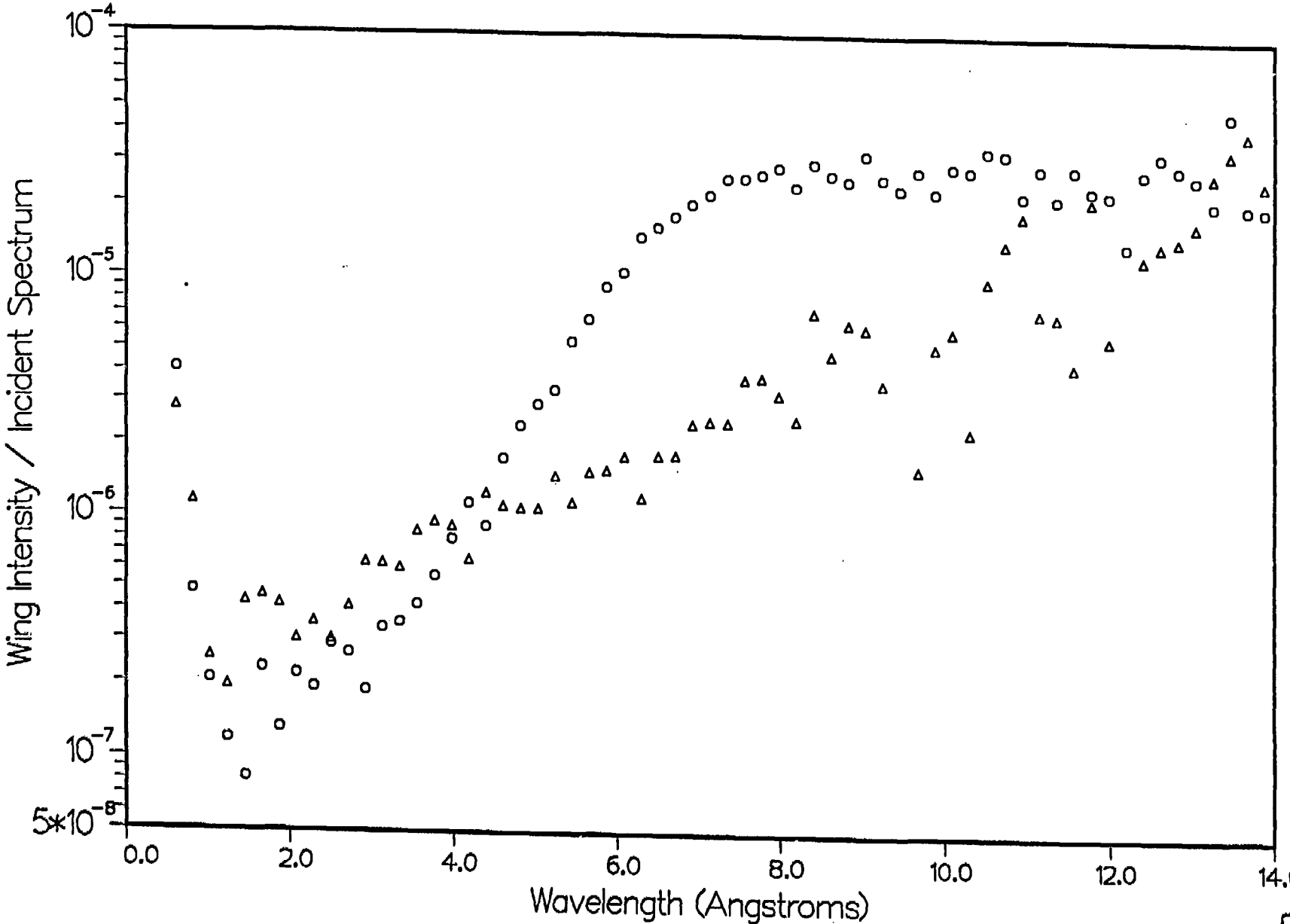
10^{-4}
10^{-5}
10^{-6}
10^{-7}
$5*10^{-8}$
Wing Intensity / Incident Spectrum
0.0
2.0
4.0
6.0
8.0
10.0
12.0
14.0
Wavelength (Angstroms)

Fig 6